# Production and Application of HPMS Recycled Bonded Permanent Magnets for a Traction Motor Application

M. Kimiabeigi, R. S. Sheridan, J. D. Widmer, A. Walton, M. Farr, B. Scholes,

I. R. Harris

***Abstract*—** Due to the volatility of the cost and sustainability concerns associated with the rare earth permanent magnets, alternative product designs using less or no rare earth contents have, recently, gained popularity. Another method to address this need is to apply a magnet recycling process, such as the novel HPMS (Hydrogen Processing of Magnetic Scrap) which can be applied to the end of life products such as Hard Drive Disks (HDDs). Despite the growing research on the background science of different recycling techniques, a practical make, use and evaluation of recycled magnets in a real life application, is rarely attended. To address this gap, in this paper and for the first time, the viability of the HPMS recycled magnets for use in a permanent magnet traction motor is investigated. On this basis, a detailed description and testing of the recycling process and the magnet production for a customized traction motor design is provided. Furthermore, the behavior of the motor using the final magnet product is analyzed using simulations and prototype testing. Based on the results, the proposed recycled magnets satisfy the overall requirements, while demonstrating similar or better electromagnetic performance compared to the alternative low cost ferrite magnets.

***Index Terms*—Ferrite Magnets, Finite Element (FE), Hydrogenation Disproportionation Desorption Recombination (HDDR), HPMS (Hydrogen Processing of Magnetic Scrap), Magnet Recycling, Traction Motor Application.**

## I. Introduction

The Rare earth permanent magnets have been utilized in high performance traction motors for many years due to their high maximum energy product, thereby, the high power density and efficiencies that can be achieved. In recent years the supply of rare earth metals has come under considerable strain due to China's dominance of the rare earth market and dramatic price fluctuations for neodymium, praseodymium and, especially, dysprosium, which are the rare earth constituents of NdFeB magnets. According to the EU Critical Materials list [1], [2] and the US Department of Energy's energy critical element list [3], the rare earth metals are classified as at greatest risk of supply shortages for clean energy technologies. As a result, research toward using cheaper grade magnets such as ferrites or NdFeB magnets with less dysprosium content has, recently, gained popularity [4, 5]. Alternatively, recycling end-of-life NdFeB magnets has been proposed as a method of ensuring a stable supply of neodymium, praseodymium and dysprosium for countries outside of China, however, at present less than 1% of rare earths are currently recycled [6, 7]. Much of the current stock of scrap NdFeB magnets is contained in the obsolete electronic and electrical equipment such as hard disk drives (HDDs). The magnets used in electric vehicles and wind turbines are expected to be in service for at least 10 and 25 years respectively, and therefore as yet, unlikely to be available in significant quantities.

It has been demonstrated that sintered NdFeB can be extracted and separated from HDDs by utilizing hydrogen as a process gas [8]. HDDs represent an ideal source of NdFeB scrap as they are relatively easy to identify, readily collected and separated from computers for secure data destruction, there is a rapid turnover of computers (~5 years) and they are the largest single application of NdFeB magnets in electronic-type goods. There are two types of NdFeB magnet in a HDD, Fig. 1: usually 2-4 fully dense sintered magnets in the voice coil motor (VCM) assembly weighing 2-30 g in total and a resin bonded magnet in the spindle motor.

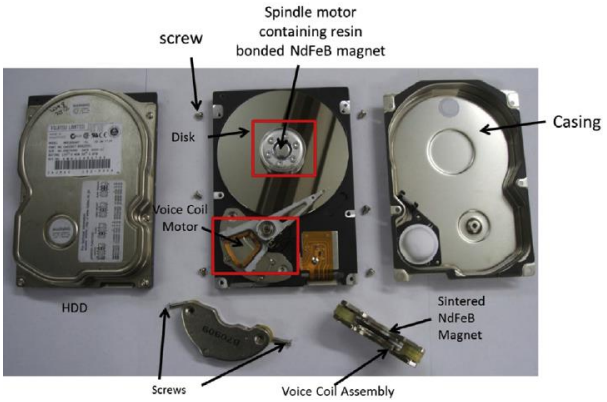


Fig. 1. A disassembled HD, displaying the spindle motor and the voice coil motor containing NdFeB magnets [8].

The method applied in the present paper, has focused on using a patented HPMS (Hydrogen Processing of Magnetic Scrap) process, [9], to recover the sintered NdFeB magnets; in this method, the NdFeB-type magnets are extracted with high

level of purity, and without damaging the remainder of the device, allowing for the recycling of the other components according to the WEEE (Waste Electronics and Electrical Equipment) legislation. In the HPMS process, the sintered NdFeB magnets are crushed and exposed to hydrogen at room temperature, at which point they undergo the Hydrogen Decrepitation (HD) process, which is already used extensively in the primary production of the rare earth magnets [10]. In the HPMS process the sintered magnet is broken down to form a friable, hydrogenated, non-coercive NdFeB powder. This hydrogenated powder is then liberated from the HDDs by mechanical agitation inside a rotating porous drum and purified using a combination of milling and sieving to remove the nickel coatings and other HDD impurities from the magnets. The purified powder can then be reprocessed in a number of different ways, such as recovering the rare earth oxides for primary production, or to re-melt for alloy production, powder processing and re-sintering, or powder processing to produce bonded magnets [8].

The recovery of the rare earths through chemical extraction techniques and re-melting has been demonstrated by multiple authors [11-15]. These techniques are less energy intensive than the primary production and allow for complete control over the composition of the final rare earth alloy. However, most re-melting is likely to be done in-house on production scrap with a known composition [16], while the solvent extraction of the rare earths is, still, energy intensive and expensive, when conducted outside China.

Direct recycling into sintered magnets has been of great interest in the last 5-10 years, where promising results, depending on the input feed of the scrap NdFeB magnets have been achieved [17, 18, 19]. These magnets require cutting into the specified shape and size, then coating for the corrosion protection (similar to the primary production), as a result of which the overall yield is reduced due to the swarf production. The recycled re-sintered magnets can provide an excellent recovery of the original material properties, but have yet to be incorporated into a commercial production stream.

An alternative method for reprocessing the recovered NdFeB powder is the production of bonded magnets. Refs [20, 21, 22] showed that it was possible to recycle scrap sintered NdFeB magnets using the hydrogenation disproportionation desorption and recombination (HDDR) process. In this work, the HD process was utilized to break uncoated NdFeB scrap magnets into a powder, similar to the HPMS process. The HDDR process was then performed at various temperatures to obtain anisotropic powder suitable for use in bonded magnets. HDDR is a high temperature hydrogen treatment that utilizes the ability of materials such as NdFeB to readily absorb and desorb hydrogen at elevated temperatures. In sintered NdFeB magnets, hydrogen is absorbed along the grain boundaries, which subsequently reacts with the Nd2Fe14B matrix phase, causing it to break down in its constituents, as shown from left to right in (1).

$$\text{Disproportionation} \rightarrow \quad Nd_2Fe_{14}B + 2xH_2 \leftrightarrow 2NdH_2x + 12Fe + Fe_2B \quad (1) \quad \leftarrow \text{Recombination}$$

The disproportionated structure is an intimate mix of NdH2 rods and finely dispersed Fe2B in an Fe matrix. The hydrogen pressure is then reduced to drive the reaction back towards the left hand side of (1), which results in recombination of the constituents back into Nd2Fe14B. The recombined matrix phase is, however, much finer than before the HDDR reaction due to the fine, intimate mixture of the disproportionated structure and the grain size is reduced from ~10 μm in the sintered magnet to ~0.3 μm in the HDDR powder. A detailed study of the development of the microstructure during the HDDR process is presented in [23]. The HDDR powder will, finally, be mixed with a polymer binder or resin, then simultaneously aligned and pressed to form anisotropic bonded magnets. As the bonded magnets can be formed into complex shapes without machining, there is little to no waste; however, the magnetic properties are lower than those of sintered magnets due to dilution by the non-magnetic binders.

The reports on the application of recycled or recyclable friendly materials into electrical machines are, mainly, limited to the replacement of the laminated steel by soft magnetic composites (SMC), where modular and/ or 3D designs become particularly favorable, [24, 25, 26]. In [27], an automated magnet disassembly concept for surface mounted magnet machines has been proposed, but the recycling and reusing of the extracted magnets have not been addressed. In [28], it is proposed that replacing the large scale magnets, in a wind power application, by a multitude of smaller size magnet blocks may minimize the magnets recycling costs with no significant compromise on the performance; however, only standard magnets (rather than recycled) were used to support the concept. In [29], a recyclable friendly epoxy free magnet arrangement, using a hermitically sealed enclosure, has been proposed and applied to a magnetic coupling device. In [30], the same magnet arrangement has been subjected to dismantling, and recycling, where further tests reveal that demagnetization of the magnet scraps via high temperatures may reduce the remanence flux density, and, more significantly, the coercivity of the recycled magnets.

In this paper, for the first time, two sets of recycled bonded type magnets based on the novel HPMS method in [9], and custom made for a specific traction motor application are manufactured, [31]. To address the literature gap on the industrial and commercial aspects of the magnets recycling, a detailed production and testing description of these magnets (from the extracted magnet scraps to the recycled finished magnet product) has been provided. Furthermore, the final magnets are tested as part of the intended traction motor application, for which both simulation and prototype testing results provide a series of performance investigation. Since the applied motor design is originally made to work with ferrite magnets [32, 33], the analyses provide a direct comparison of the proposed recycled magnets practicality against the already established low cost ferrite magnet alternative.

## II. Traction Application Requirement

To implement the proposed recycled magnets concept, an electric boat traction motor application, with the design requirements in Table I and Fig. 2, [34], has been considered.

Due to the similarity of the recycled magnets remanence flux density and the coercivity levels to that of the ferrite magnets, FB9B, and to enable a direct comparison of the two magnet types based on a similar size and motor design, a scaled version of an existing spoke type ferrite magnet motor, [32], has been chosen for the purpose.

TABLE I
DESIGN REQUIREMENTS FOR AN ELECTRIC BOAT TRACTION APPLICATION.

| | |
|---|---|
| Available volume (Inc. end winding; Exc. housing) | > 10 liter |
| Maximum winding temperature | 155 ˚C/ Class F |
| Maximum magnet temperature | 130 ˚C |
| Cooling | Passive convection |
| Maximum inverter current, $I_{pk}$ | 200 Arms |
| Nominal available DC link voltage | 48 V |
| Demagnetization resistance | 3-phase short circuit |
| Recycled magnet (V1) Br at 20˚C/ $H_{cj}$ at 20˚C | 0.43 T/ 700 kA/m |
| Recycled magnet (V2) Br at 20˚C/ $H_{cj}$ at 20˚C | 0.6 T/ 950 kA/m |
| Ferrite FB9B magnets Br at 20˚C/ $H_{cj}$ at 20˚C | 0.43 T/ 370 kA/m |
| Stator and rotor laminations | M27035A Silicon steel |

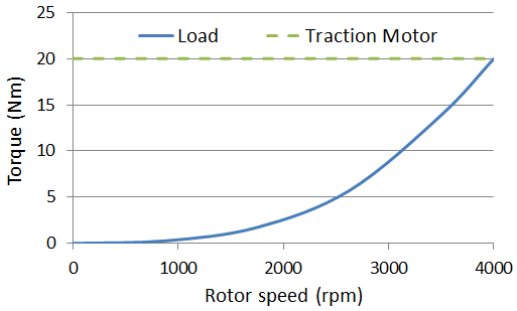


Fig. 2. Torque-speed profile required by the electric boat, and the matching traction motor output, at 20 °C.

## III. MANUFACTURING OF RECYCLED MAGNETS

### A. HDDR Process

Throughout this work, uncoated scrap sintered NdFeB-type magnets with the composition Nd13.4Dy0.7Fe78.6Al0.7Nb0.4B6.2 (trace elements not included, atomic % measured by ICP analysis) with an oxygen content of 2665 ppm (measured by LECO analysis) have been used. The scrap magnets have been loaded into a specially designed hydrogen decrepitation chamber. Hydrogen is introduced to 2 bar absolute pressure and held for two hours until the HD process is complete, before evacuating to ~$10^{-2}$ mbar.

The HDDR processing utilized in this paper can be described as follows [22]: The HD powdered sample, which is extracted during the HPMS process, is transferred inertly to a vacuum sintering furnace tube (designed for use with argon, hydrogen or vacuum) and evacuated to ~$10^{-2}$ mbar. The sample is then heated to 885 ºC under vacuum to degas the hydrogen absorbed during the HD process. Hydrogen is then introduced at a rate of 16 mbar min-1 up to 1500 mbar, and held for 30 minutes to ensure complete disproportionation. The hydrogen pressure is then reduced at 100 mbar $min^{-1}$ to a vacuum, and held until reaching a pressure of ~$10^{-2}$ mbar in order to complete the recombination process. The furnace is then rolled off the furnace tube to encourage quick cooling of the sample. Fig. 3 shows a schematic representation of the complete HDDR process. Due to the system volume limitations the HDDR process is split over two batches, the hysteresis loops in the 'easy' direction of magnetization of both batches are shown in Fig. 4, which demonstrates an excellent reproducibility.

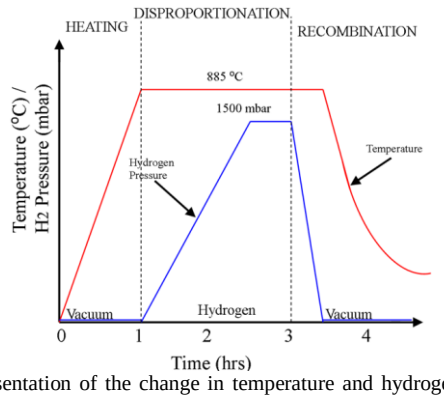


Fig. 3. Representation of the change in temperature and hydrogen pressure with respect to time throughout the HDDR process.

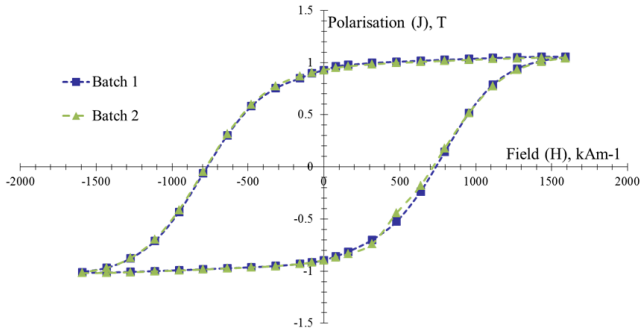


Fig.4. Hysteresis Loops in the 'easy' directions of magnetization for the two batches of HDDR powder, measured using a vibrating sample magnetometer.

The coarse magnet powder obtained by HDDR is burr-milled to reduce the particle size to <150 µm. The milled powders are, then, mixed with the fine Poly Tetra Fluoro Ethylene (PTFE) powder using a ratio of (2), where wt% correspond to the weight in percentage.

$$80\ \text{wt\%}\ Nd_2Fe_{14}B : 20\ \text{wt\%}\ \text{PTFE} \qquad (2)$$

The two components are combined in a plastic pot and loaded with ball bearings and mixed for 5 minutes to allow even distribution of the PTFE throughout the structure. These are, then, ready for pressing into net-shape compacts using a specially designed easy-release die set in a uniaxial press (10 tons) with a transverse magnetic field gradient across the sample, Fig. 5. The pressed compacts are ejected from the die set, transferred to a vacuum sintering furnace in order to cure the PTFE. The samples are heated to 360 °C and held for 5 minutes before slow furnace cooling to the room temperature to cure the PTFE binder. The magnets in their final shape and with half and one third of the nominal length, i.e. ~ 19.5 mm and 13 mm, are shown in Fig. 12(a).

A problem realized during the manufacturing process is that due to the softness of the aluminum inserts compared to the steel punch piece, any distortion during the pressing, such as

misalignment, could result in scratch and damages of the insert inner faces, Fig. 5(c). This phenomenon will cause the magnets geometrical tolerance deviate from the specifications, and might deteriorate with the number of magnets produced. To resolve the issue for a high volume production, inserts made of harder material, such as stainless steel or bronze, need to be made, which are currently under investigation.

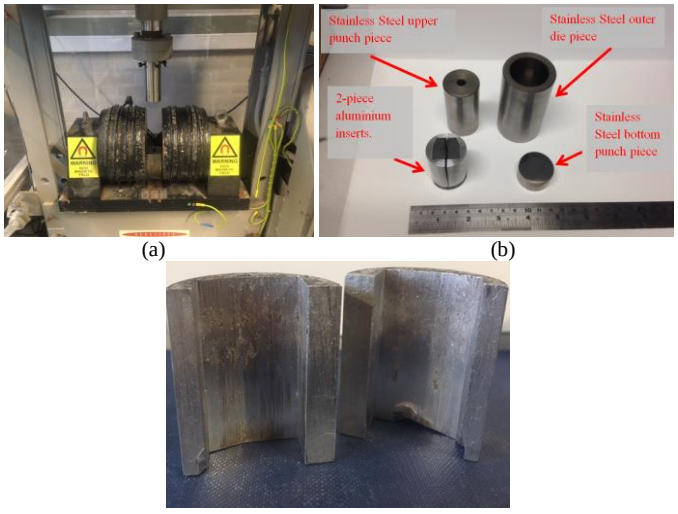


Fig.5. The uniaxial press set up with a transverse field electromagnet. (a) Pressing tool, including the punch piece and the electromagnet coil. (b) Die set and punching components. (c) Die set inner face damages due to pressing misalignment.

### *B. Magnet Segmentation and the Influence on the Magnetic Properties*

During the course of this work, two sets of bonded magnets, namely V1 and V2, have been produced. For the first set, the nominal 39 mm total required length of the magnets was split, axially, over two magnets (i.e. 19.5 mm each) to allow for a complete compaction of the magnet powder/binder mixture within the allocated die set volume. The subsequent bonded magnets were tested using a standard closed-loop permeameter set up, and exhibited a remanence of 0.43 T and intrinsic coercivity of 700 kA/m. These magnetic properties were much lower than expected from the HDDR powder, and, as will be reported in Section IV, the electromagnetic performance of the motor under testing was below the requirements for the specified traction application. It was determined that due to the high fill factor of the die, compression of the powder/binder mix was occurring in the die during the loading, which prevented the particles from rotating in the applied magnetic field during pressing, resulting in lower magnetic properties. For the second set of magnets, the nominal 39 mm total required length was split over three magnets (i.e. 13 mm each) to prevent a pre-compaction in the die during the loading, and allow for a free rotation of the particles during the magnetic alignment and pressing. The demagnetization curves of three sample magnets taken, at random, from the resultant batch are shown in Fig. 6. It can be observed that there is an excellent reproducibility across the three magnets, while an improved remanence of 0.6 T and intrinsic coercivity of 950 kA/m have been achieved. The pre-compaction concept and its implication have been illustrated in Fig. 7.

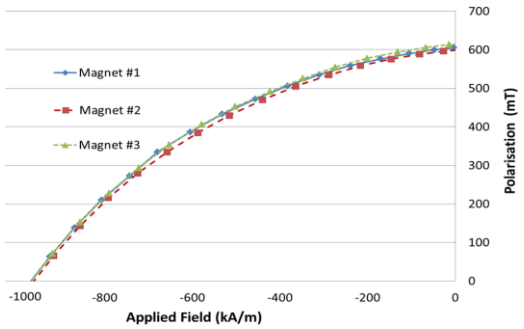


Fig.6. Demagnetization loops of three sample magnets taken at random from V2 set of magnets, measured using a closed-loop permeameter.

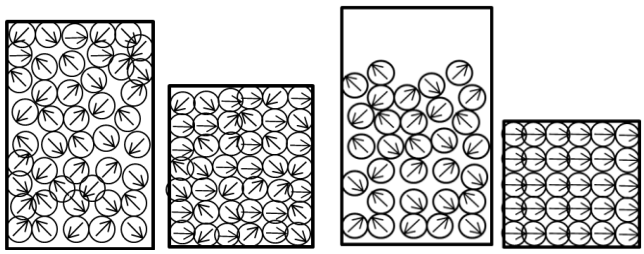


Fig.7. Illustration of magnetic grain alignment under the influence of mechanical pre-compaction. (a) Randomly aligned particles with pre-compaction → 1/2 desired length with poor grain alignment. (b) Randomly aligned particles without pre-compaction → 1/3 desired length with excellent grain alignment.

## IV. Motor Design Analysis

The HDDR recycled magnets produced in Section 3, are fitted into a traction motor design, which is a one-fifth scale down of a design, originally, intended for use with ferrite magnets [32]. The design is consisted of a spoke type single piece rotor, [33], and a distributed wound stator. The main geometrical dimensions of the design have been summarized in Table II. The electromagnetic, thermal and structural performance of the motor will be investigated in the following sections.

TABLE II
GEOMETRICAL DIMENSIONS OF THE TRACTION MOTOR DESIGN.

| | |
|---|---|
| Stator outer diameter (mm) | 205 |
| Rotor outer diameter (mm) | 140 |
| Stack length (mm) | 39 |
| Airgap (mm) | 0.5 |

### *A. Electromagnetic Torque*

The magnetic flux and the field distribution based on magnets V2, see Table I, and during the peak power operation is calculated in FE 2D, and shown in Fig. 8(a). From Fig. 8(a), the effectivity of the rotor yoke bridges in reaching an early level of saturation, thereby limiting the magnetic leakage, is demonstrated.

The peak electromagnetic torque at 4000 rpm, and using both versions of recycled magnets, is simulated and shown in Fig. 8(b). Based on Fig. 8(b), as a result of increasing the

magnet $B_r$ by 40%, i.e. V2 vs. V1 magnets, the average torque has increased by about 50%, which is due to the combined effects of the magnet and reluctance based torque components. The increase of the reluctance torque component is due to the improved saliency as a result of the higher contribution of the stronger V2 magnets in saturating the rotor yoke posts and bridges, thereby reducing the leakage via the d-axis component of the armature reaction field. To confirm this, the direct and the quadrature axis inductances, $(L_q, L_d)$, with both magnet types and at the maximum torque conditions, i.e. 200 Arms, have been calculated in FE 2D and obtained equal to (35 µH, 21 µH) for V1 type and (35 µH, 19 µH) for V2 type magnets, indicating a 14% rise of the saliency ratio, $(L_q - L_d)$, and the reluctance torque in favor of the V2 type magnets. Finally, from Fig. 8(c), a 20% (~ 2 Nm) increase of the ripple torque for the stronger V2 type magnets is obtained.

The motor terminal voltages at the peak power operation, and based on both grades of magnets, have been simulated and shown in Fig. 8(d). Based on Fig. 8(d), despite the 40% stronger $B_r$ of the V2 magnets compared to the V1 magnets, the fundamental voltage amplitude of the corresponding design is only 10% higher. This behavior is due to the lower armature reaction voltage (in particular the voltage component associated with the direct axis leakage inductance) of the design using the V2 magnets, which, itself, is due to the more effective saturation of the rotor yoke bridges achieved by the stronger magnets.

The described findings on the torque and voltage, demonstrate that in a motor design with a spoke type rotor and a single piece rotor topology, where the d-axis inductance is, inversely, affected by the magnets strength (via magnetic saturation), a substantial enhancement of the torque and power density using stronger magnets, can be achieved.

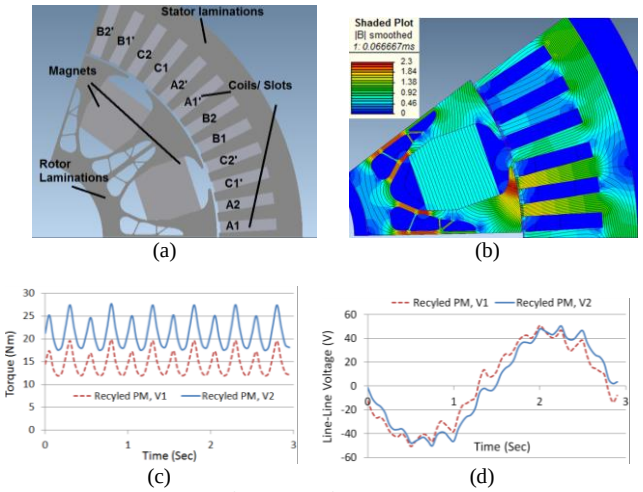


(a) (b) (c) (d)

Fig.8. Electromagnetic performance of the traction motor using two versions of recycled magnets. (a) 2D Cross section of the motor model. (b) Magnetic field and flux distribution under peak power loading, using magnets V2. (c) Comparison of maximum electromagnetic torque obtained by magnets V1 and V2. (d) Comparison of terminal voltage, at peak power loading, obtained by magnets V1 and V2.

## B. *Demagnetization*

To assess the demagnetization resistance performance of the applied magnets, a three phase short circuit fault during a peak power operation, 200 Arms with 40° Advance Angle at 4000 rpm (corresponding to the motor operation at the maximum energy level and the worst case scenario) has been investigated. From Fig. 9(a), the peak fault current of 215% of the peak rated current may occur, for which the magnetic field and flux vectors in the magnets have been simulated in Fig 9(b). From Fig. 9(b), it can be realized that the magnetic field in the magnets regions does not exceed 190 kA/m, which is, safely, below the intrinsic coercivity of the V2 magnets at the room temperature, Table I, as well as their estimated coercivity at 130 °C of 323 kA/m, assuming a $H_{cj}$ temperature coefficient of -0.6%/°C (based on the available values for the sintered HPMS magnet types). Alternatively, it can be observed that the flux vectors, throughout the magnet cross section, retain the intrinsic magnet polarity, implying a safe operation under the demagnetization fault.

With regards to the V1 magnets, it should be noted that similar results and conclusions have been obtained, where the maximum field in the magnets is, safely, below 238 kA/m, which is the estimated coercivity of the magnets at 130 °C.

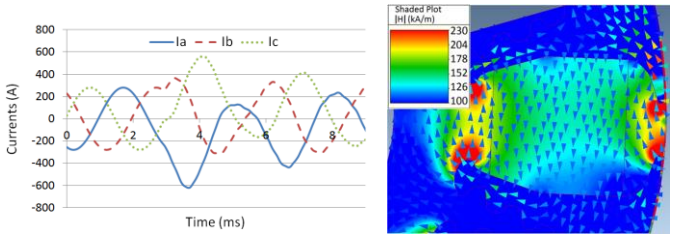


(a) (b)

Fig.9. Performance of the traction motor design under short circuit and demagnetization conditions. (a) The motor terminal currents under peak power operation followed by a 3-phase short circuit, magnet V2. (b) Magnetic field and flux distribution during worst instant of demagnetization conditions, magnet V2.

## C. *Efficiency and Thermal Analysis*

The electromagnetic efficiency of the proposed traction motor under the full torque-speed envelope, accounting for the winding and the iron losses, has been simulated using a coupled analytical-FE based method, [35], and shown in Fig. 10(a); the AC loss part of the windings proved to be negligible due to the optimal disposition of the parallel wires inside the slots [36]. From Fig. 10(a), an efficiency of 94% is achieved at the peak power operating point, whilst due to a constant torque vs. speed nature of the motor design, Fig. 2, the efficiency is, generally, improved by increasing the rotor speed (as the output power is increased, the losses are, mainly, driven by constant current amplitudes, thereby, not changing as much).

The temperature response of the motor under the peak power operation, an ambient temperature of 20 °C, and assuming a passive convective cooling through the stator housing fins has been calculated based on a lumped network method in Motor Cad [37], and shown in Fig. 10(b). From Fig. 10(b), the proposed motor design can deliver the predicted electromagnetic peak power of 8.8 kW (21 Nm at 4000 rpm) continuously, with the temperatures of the windings and the magnets staying below the specified limits in Table I.

Finally, to assess the performance depreciation at higher temperatures, the efficiency map at the hottest operation

condition, i.e. 130°C magnet and 150 °C winding temperature according to Fig. 10(b), have been simulated and shown in Fig. 10(c). From Fig. 10(c), due to the loss of $B_r$ and higher winding resistance, a 4~5% reduction of efficiency and ~30% reduction of torque density is obtained.

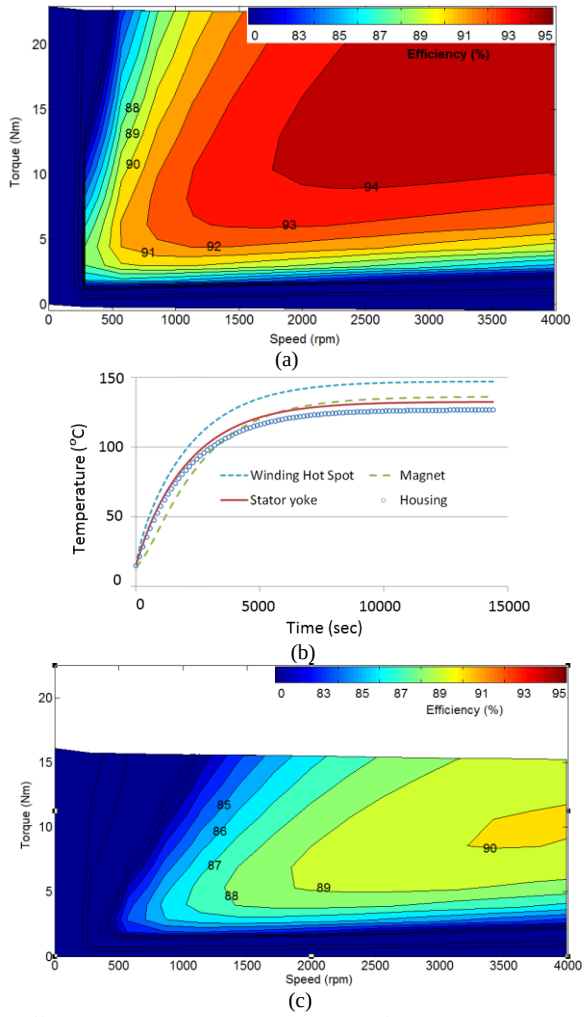


Fig.10. Efficiency map and the thermal response of the traction motor with V2 recycled magnets. (a) Efficiency map at 20 °C. (b) Thermal response under peak power loading, 20 °C ambient temperature. (c) Efficiency map at 130°C magnet and 150 °C winding temperature.

## D. *Structural Analysis*

The rotor topology of the proposed motor design is obtained based on a novel stress-constrained mass minimization technique, [33], and is, originally, designed against a more strict structural requirement, i.e. up to a 15000 rpm maximum speed. The stress distribution at 15000 rpm using a structural finite element analysis is shown in Fig. 11, where the peak stress of 299 MPa is, safely, below the yield strength of the selected rotor lamination material, i.e. M270-35A.

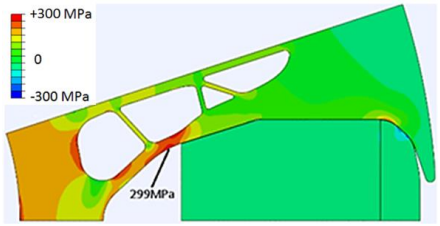


Fig.11. Stress distribution at 15000 rpm of the proposed traction rotor design.

## E. *Prototype Testing*

To validate the performance of the proposed traction motor design using the recycled magnets, a prototype testing using both grades of magnets has been conducted, Fig. 12.


Fig.12. Prototype traction motor using recycled magnets. (a) Rotor, with display of the recycled magnets, V1 and V2, and a full size ferrite magnet. (b) Assembled rotor with recycled magnets, V1. (c) Wound stator.

The BEMF and static torque of the prototype motor under the ambient temperature of 20 °C have been measured and compared against the FE simulations in Figs. 13 and 14. From Fig. 13, the measured BEMF (considering the fundamental component) is 6% and 9% lower than the predictions, which can be, partly, attributed to the under-sized magnets due to the manufacturing tolerances, Section III, and partly due to the 3D leakage due to the short length of the stack compared to the airgap diameter. With regards to the static torque, Fig. 14, a similar behavior as for the BEMF can be observed, where a maximum deviation of 9% and 12% for V1 and V2 magnets have been obtained, respectively; the deviation is due to the combined deviations in the BEMF and the 3D leakage of the armature reaction.

To evaluate the recycled magnets against the conventional ferrite magnets, the prototype motor in Fig 12 with FB9B ferrite magnets has been tested, which provides an identical performance to that of the V1 recycled magnets. This has been expected due to the identical $B_r$ of the two magnet types at the room temperature, and confirms that the recycled bonded magnets (with suitable quality levels, such as V2 grade) may provide higher torque densities than the best available grade of ferrite magnets, such as the FB9B in this paper.

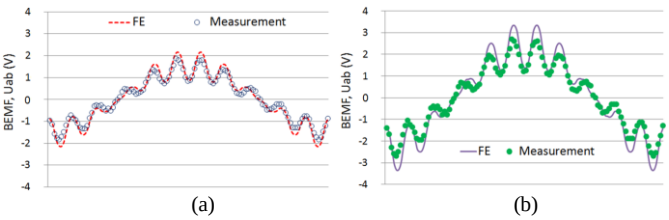


Fig.13. Comparison of BEMF from prototype measurement and FE simulations, 400 rpm. (a) Recycled magnet V1. (b) Recycled magnet V2.

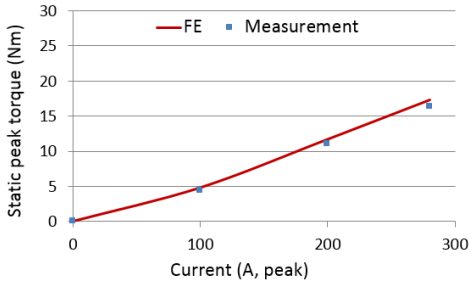


(a)

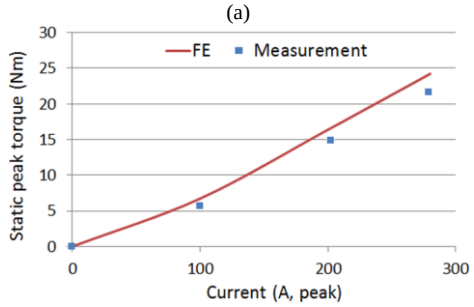


(b)

Fig.14. Comparison of electromagnetic torque from prototype measurement and FE simulations. (a) Traction motor using recycled magnet V1. (b) Traction motor using recycled magnet V2.

To evaluate the temperature influence on the recycled magnets, the maximum static torque of the prototype motor (200 Arms) using V2 recycled, as well as the ferrite magnets has been measured, and compared against the FE simulations (where a $B_r$-temperature coefficient of -0.3%/ ˚C is assumed) , Fig 15. Based on the measured data points in Fig. 15 for the recycled magnets, a coefficient of -0.28%/ ˚C is obtained, which is closely consistent with the theoretical assumptions. Furthermore, it can be noted that the recycled magnets $B_r$, thereby torque contribution, is more sensitive to the higher temperatures, and drops more quickly compared to their counterpart ferrite magnets.

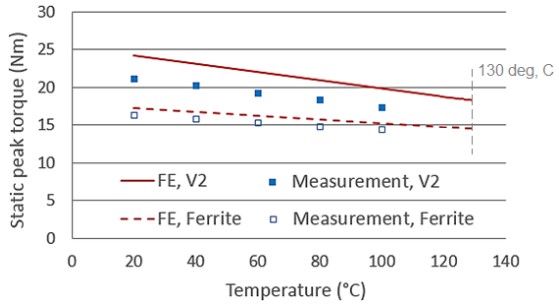


Fig.15. Static peak torque vs. magnet temperature: a comparison of the motor designs with recycled, V2, and ferrite magnet.

To validate the magnets performance during dynamic conditions, the prototype motor using both recycled V2 and ferrite magnets and at two different operating temperatures has been run at maximum torque and up to 2000 rpm. The winding temperatures are monitored through thermocouples fixed to the end coils, whilst the magnet temperatures are estimated based on the winding temperature and the thermal simulation (using Motor Cad [37]) set up to the loading conditions. The measurement results including the torque and efficiency data are shown and compared against the FE simulation data in Fig. 16. From Fig. 16, whilst a consistent agreement between the measured and the simulation data is achieved, the superiority of the V2 magnets compared to the ferrite magnets in terms of both torque density and efficiency is confirmed. Furthermore, as demonstrated in case of static testing, due to the higher susceptibility of the recycled magnets $B_r$ to the temperatures compared to the ferrite magnets, the performance gap between the two drops at higher temperatures.

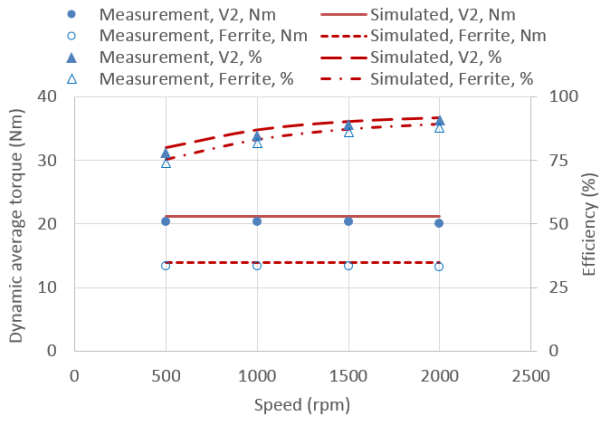


(a)

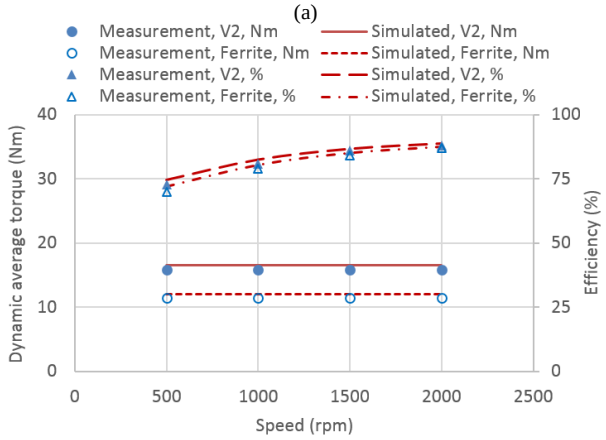


(b)

Fig.16. Dynamic torque and efficiency testing of the prototype motors with the recycled V2 and ferrite magnets. (a) Magnet at 40 ˚C and winding at 70 ˚C. (b) Magnet at 100 ˚C and winding at 120 ˚C.

Finally, with regards to the demagnetization, several tests applying different amplitudes of currents, and using both ferrite and recycled V2 magnets have been conducted. Matching the theoretical expectations, Section IV.B and accounting for the additional 3D effects associated with the short length prototype design, [38], both magnets showed excellent demagnetization resistance (i.e. zero changes of $B_r$ and BEMF) against fault currents as large as 600A, i.e. > 200% of the rated current.

## V. Commercial Viability

Based on the successful production and testing of the proposed HPMS recycled magnets in this paper, it is anticipated that these magnets can serve as a suitable alternative solution to replace non-recycled (primary) rare earth magnets. To encourage this commercial viability, a breakdown of the magnet production costs as well as a comparison with the ferrite magnets in terms of the cost and

performance have been provided in Fig. 17 and Table III. With regards to Fig. 17, it should be noted that by rising the raw rare earth material cost (e.g. during the peak price time of 2011-2012) and/ or the production/ order volume, the initial material cost element will grow in terms of the percentage over the final magnet product cost. As a result, based on the historical and the current prices of the rare earth metals and the non-recycled (primary) magnet costs, [39, 40], it can be concluded that the rare earth material cost would form a dominant part of the final magnet product cost during the high price cycles and/ or when a global demand is considered. On this basis, since the initial material costs associated with the proposed HPMS recycled magnets is zero, with the possibility of being negative (subject to the governmental subsidies), it is estimated that despite the more complex fabrication process, the recycled magnets have the potential of coming in stable prices, which can be lower than the non-recycled (primary) rare earth magnets, and competitive to that of the ferrite magnets, Table III.

With regards to the performance and measured against the highest grades of ferrite magnets, Table III, the recycled magnets can demonstrate higher torque capability, higher efficiency (due to higher magnetic loading), and similar demagnetization resistance at the extreme temperatures (ferrite and NdFeB magnets have opposite trends of coercivity against temperature). On this basis, a direct replacement (or marginal adaptation) of the ferrite based motor designs using the proposed HPMS recycled magnets is envisaged.

Further comparisons of the low cost traction motors against the conventional rare earth motors, such as Nissan Leaf have been presented in [33], [36] and [41].

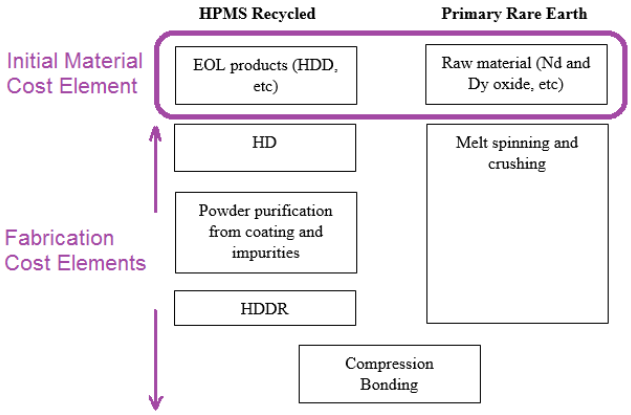


Fig.17. A breakdown of the HPMS recycled vs. non-recycled (primary) magnets production and cost elements.

TABLE III
AN ILLUSTRATIVE COMPARISON OF THE HPMS RECYCLED AND FERRITE MAGNETS.

| | Torque/ Power density (per unit) | Peak Efficiency | Demagnetization Withstand ($H_{cj}$) | Cost (per unit) |
|---|---|---|---|---|
| Ferrite (FB9B) | 1 | ~ η% | 310 kA/m @ -40 ˚C | 1 |
| HPMS Recycled Magnet (V2) | 1.2-1.4 | ~ η +1% | 323 kA/m @ +130 ˚C | 1<k<<x* (*primary rare earth) |

## VI. CONCLUSIONS

In this paper, for the first time in the literature, a detailed description of the production and testing process of a HPMS recycled bonded magnet for a custom built traction motor application has been provided. Due to the choice of a proven traction motor design based on ferrite magnets, the analyses provide a direct assessment of the proposed recycled magnets against the former having an identical size/ volume and comparable magnetic properties. During the course of the magnet production, it is realized that a mechanical pre-loading may hinder the magnet particles free alignment, resulting in a, significantly, poorer magnetic BH data, i.e. $B_r$ and $H_{cj}$. Furthermore, the choice of the pressing and the insert tools surface roughness can have a significant impact on the magnets geometrical tolerance, which, in turn, may influence the motor performance, and the possibility for a high volume production.

Through a series of multi-physical simulations, prototype testing, and comparison against the low cost ferrite magnets, it was demonstrated that not only the proposed HPMS recycled magnets has the potential to fulfil traction motor requirements, they may provide higher torque density, higher efficiency, and similar demagnetization performance as the ferrite magnets. Furthermore, targeting a high volume production (subject to future global demand) and during a high price cycle of the rare earth materials, they can come in competitive prices, which can be as low as a fraction of the non-recycled NdFeB magnets and, even, competitive to those of the low cost ferrite magnets.

## REFERENCES

[1] Critical Raw Materials for the EU, 2010. European Commission, Brussels, Belgium.
[2] Critical Raw Materials for the EU, 2014. European Commission, Brussels, Belgium.
[3] Critical Materials Strategy, 2011, US Department of Energy.
[4] D. Dorrell, L. Parsa, and I. Boldea, "Automotive electric motors, generators, and actuator drive systems with reduced or no permanent magnets and innovative design concepts," IEEE Trans. On Indus. Elects, 2014, vol. 61, no. 10, pp 5693 – 5695.
[5] J. Widmer, R. Martin, and M. Kimiabeigi, "Electric vehicle traction motors without rare earth magnets," Sustainable Materials and Technologies (Elsevier), 2015, vol. 3, pp 7-13.
[6] K. Binnemans, P.T. Jones, B. Blanpain, *et al,* "Recycling of rare earths: a critical review', Journal of Cleaner Production, 2013, vol. 51, pp 1-22.
[7] Y. Yang, A. Walton, R. Sheridan, *et al*, "REE recovery from end-of-life NdFeB permanent magnet scrap: a critical review," Springerlink.com, 2016, DOI: 10.1007/s40831-016-0090-4.
[8] A. Walton, H. Yi, N.A. Rowson, *et al,* "The use of hydrogen to separate and recycle Neodymium-iron-boron-type magnets from electronic waste," Journal of Cleaner Production, 2015, vol. 104, pp 236-241.
[9] "Magnet recylcing,'' by I.R.Harris, A. Williams, A. Walton, J. Speight, Granted on May 2014, US8734714 B2, Available: http://www.google.co.uk/patents/US8734714.
[10] P.J. McGuiness, I.R. Harris, E. Rozendaal, *et al*, "The production of a Nd-Fe-B permanent magnet by a hydrogen decrepitation/ attritor milling route," Journal of Materials Science, 1986, vol. 21, pp 4107.
[11] C.O. Bounds, "The recycle of sintered magnet swarf," Symposium on Metals and Materials Waste Reduction, Recovery and Remediation, Rosemont, 1994, pp. 173–186.
[12] T.W. Ellis, F.A. Schmidt, L.L. Jones, "Methods and opportunities in the recycling of rare earth based materials," Symposium on Metals and Materials Waste Reduction, Recovery and Remediation, Rosemont, 1994, pp. 199–2006.

[13] Y. Baba, F. Kubota, N. Kamiya, *et al*, "Recent advances in extraction and separation of rare-earth metals using ionic liquids," Journal Chemical Engineering, Japan, 2011, vol. 44, pp. 679–685.

[14] Suzuki, R.O., Saguchi, A., Takahashi, W., et al.: 'Recycling of rare earth magnet scraps: Part II Oxygen removal by calcium', Material Transactions, 2001, vol. 42, pp. 2492–2498.

[15] A. Saguchi, K. Asabe, W. Takahashi, *et al*, "Recycling of rare earth magnet scraps: part III carbon removal from Nd magnet grinding sludge under vacuum heating," Material Transactions, 2002, vol. 43, pp. 256–260.

[16] M. Tanaka, T. Oki, K. Koyama, *et al*, "Recycling of rare earths from scrap," Handbook on the Physics and Chemistry of Rare Earths, Elsevier, 2013, vol. 43, pp. 159–211.

[17] M. Zakotnik, I.R. Harris, A.J. Williams, "Possible methods of recycling Nd–Fe–B-type sintered magnets using the HD/degassing process," Journal of Alloys & Compounds, 2008, vol. 450, pp. 525–531.

[18] M. Zakotnik, I.R. Harris, A.J. Williams, "Multiple recycling of Nd–Fe–B-type sintered magnets," Journal of Alloys & Compounds, 2009, vol. 469, pp. 314–321.

[19] A. Walton, Y. Han, V.S. Mann, *et al* "The use of hydrogen to separate and recycle Nd–Fe–B magnets from electronic waste," 22nd International Workshop on Rare Earth Magnets and their applications, Japan, 2012, pp 10-13.

[20] R.S. Sheridan, R. Sillitoe, M. Zakotnik, *et al*, "Anisotropic powder from sintered NdFeB magnets by the HDDR processing route," Journal of Magnetism & Magnetic Materials, 2012, vol. 324, pp 63-67.

[21] O. Gutfleisch, K. Guth, T.G. Woodcock, *et al*, "Recycling used Nd-Fe-B sintered magnets via a hydrogen-based route to produce anisotropic, resin bonded magnets," Journal of Advanced. Energy Materials, 2013, vol. 3, pp 151-155.

[22] R.S Sheridan, A.J. Williams, I.R. Harris, *et al*, "Improved HDDR processing route for production of anisotropic powder from sintered NdFeB type magnets," Advanced Journal of Magnetism & Magnetic Materials, 2014, vol. 350, pp 114-118.

[23] R.S. Sheridan, I.R. Harris, A. Walton, "The development of microstructure during hydrogenation–disproportionation–desorption-recombination treatment of sintered neodymium-iron-boron-type magnets," Journal of Magnetism & Magnetic Materials, 2016, vol. 401, pp 455–462.

[24] S.T. Lundmark, and M. Alatalo, "A segmented clawpole motor for Traction Applications Considering Recycling Aspect," 8th International Conference and Exhibition on Ecological Vehicles and Renewable Energies (EVER), Monaco, 2013, DOI: 10.1109/EVER.2013.6521613.

[25] C. Henaux, B. Nogarede, and D. Harribey, "A new concept of modular permanent magnet and soft magnetic compound motor dedicated to widespread application," IEEE Trans. Magn., 2012, vol. 48, no. 6, pp. 2035–2043.

[26] M. Alatalo, S. Lundmark, and E. Grunditz, "Electric machine design for traction applications considering recycling aspects—Review and new solution," in Proc. IEEE IECON, 2011, pp. 1836–1841.

[27] T. Klier, F. Risch, and J. Franke, "Disassembly, recycling, and reuse of magnet material of electric drives," in 2013 IEEE International Symposium on Assembly and Manufacturing (ISAM), 2013, pp. 88–90.

[28] S. Hogberg, T.S. Pedersen, F.B. Bendixen, "Direct Reuse of Rare Earth Permanent Magnets Wind Turbine Generator Case Study," XXII International Conference on Electrical Machines (ICEM), 2016, pp. 1625-1629, DOI: 10.1109/ICELMACH.2016.7732741

[29] S. Hogberg, N. Mijatovic, J. Holbøll, *et al*, "Parametric design optimization of a novel permanent magnet coupling using finite element analysis," Energy Conversion Congress and Exposition (ECCE), 2014, pp. 1465–1471.

[30] S. Hogberg, F.B. Bendixen, N. Mijatovic, *et al*, "Influence of demagnetization-temperature on magnetic performance of recycled Nd-Fe-B magnets," In proceeding of the IEEE international electric machines and drives conference (IEMDC), 2015, pp 1242–1246.

[31] M. Kimiabeigi, J. D. Widmer, R. S. Sheridan, A. Walton A, R. Harris, "Design of high performance traction motors using cheaper grade of materials," Proceedings of 8th IET International Conference of Power Electronics, Machines and Drives (PEMD)., April 2016, DOI: 10.1049/cp.2016.0287.

[32] M. Kimiabeigi, J. Widmer, R. Long, *et al,* "High Performance Low Cost Electric Motor for Electric Vehicles Using Ferrite Magnets," IEEE Trans. Ind. Electron., 2016, vol. 63, no. 1, pp.113-122.

[33] M. Kimiabeigi, R. Long, J. Widmer, Y. Gao, "Comparative Assessment of Single Piece and Fir Tree Based Spoke Type Rotor Designs for Low Cost Electric Vehicle Application," IEEE Trans. Energy. Convers., Feb 2017, DOI: 10.1109/TEC.2017.2662579.

[34] G. Theotokatos, and V. Tzelepis, "A Computational Study on the Performance and Emission Parameters Mapping of a Ship Propulsion System," Proc. Inst. Mech. Eng. Part M: J. Eng. Marit. Environ., 229(1), Jan 2013, pp. 58–76.

[35] J. Goss, P. H. Mellor, R. Wrobel, D. A. Staton, and M. Popescu, "The design of AC permanent magnet motors for electric vehicles: a computationally efficient model of the operational envelope," in 6th IET International Conference on Power Electronics, Machines and Drives (PEMD 2012), 2012, pp. B21–B21.

[36] M. Kimiabeigi, J. Widmer, "On winding design of a high performance ferrite motor for traction application," XXII International Conference on Electrical Machines (ICEM), 2016, DOI: 10.1109/ICELMACH.2016.7732790.

[37] D.A. Staton, "Thermal computer aided design—Advancing the revolution in compact motors," in Conf. Rec. IEEE-IEMDC, Boston, MA, Jun. 2001, pp. 858–863.

[38] M. Kimiabeigi, J. D. Widmer, R. Long, *et al*, "3D Modelling of Demagnetization and Utilization of Poorer Magnet Materials for EV/ HEV Applications," IEEE Trans. Energy. Convers., Sep 2016, vol. 31, no. 3, pp.981-992.

[39] China rare earth magnet ltd. [Online]. Available: http://www.permanentmagnet.com/price-trend-of-rare-earth-neodymium-material.html

[40] Mineral fund advisory pty. ltd. [Online]. Available: http://mineralprices.com/default.aspx#rar

[41] M. Kimiabeigi, J. D. Widmer, R. Long, Y. Gao, J. Goss, R. Martin, T. Lisle, J.M. Soler Vizan, A. Michaelides, and B. Mecrow, "On Selection of Rotor Support Material for a Ferrite Magnet Spoke Type Traction Motor," IEEE Trans. Ind. Appl., vol. 52, no. 3, pp.2224-2233, May/ June 2016.